Silver Nanoparticles Supported Graphitic Like Carbon Nitride for the Electrochemical Sensing of Nitrobenzene and its Derivatives

Pandiyarajan C (cpandiyarajanchem@gmail.com)
Madurai Kamaraj University https://orcid.org/0000-0003-2851-2377
Rameshkumar Perumal
Kalasalingam Academy of Research and Education
Murugesan S
Madurai Kamaraj University
Selvaraj M
King Khalid University

Research Article

Keywords: Electrocatalysis, g-C3N4 nanosheets, Nanocomposites, Nitrobenzene sensor, Silver nanoparticles

Posted Date: June 22nd, 2021

DOI: https://doi.org/10.21203/rs.3.rs-167924/v1

Version of Record: A version of this preprint was published at Journal of Materials Science: Materials in Electronics on July 6th, 2021. See the published version at https://doi.org/10.1007/s10854-021-06515-z.

Abstract

Nitrobenzene (NB) is toxic even at low concentrations and hence, its contamination in the environment is a pervasive concern. The electrochemical techniques have emerged as rosy method to sense and degrade NB and graphitic carbon nitride (g-C_3N_4) catalysts are found to be promising for this. In this study, silver nanoparticles (AgNPs) decorated N-[3-(trimethoxysilyl)propyl]ethylenediamine (EDAS) modified graphitic carbon nitride nanocomposites (EDAS/(g-C_3N_4-Ag)$_{NC}$) having various silver concentrations are prepared through a facile method and applied for the electrochemical sensing of NB derivatives. UV-vis absorption edge at 430 nm together with a broad surface plasmon resonance (SPR) peak at 450 nm indicates the existence of AgNPs on the g-C_3N_4 nanosheets. FT-IR spectra endorse the presence of g-C_3N_4 nanosheets in the composite. The presence of Ag in EDAS/(g-C_3N_4-Ag)$_{NC}$ is confirmed by transmission electron microscopy, energy dispersive X-ray analysis and cyclic voltammetry (CV). The nanocomposite prepared with 2 mM Ag^+ shows superb electrocatalytic activity towards the reduction of nitrobenzene and its derivatives. Sensitivity of the modified electrode and limit of detection (LOD) for NB assessed by square wave voltammetry are found to be 0.594 A M^{-1} cm^{-2} and 2 μM, respectively, in the linear range of 5–50 μM.

1. Introduction

Mutagenic and carcinogenic behavior of nitroaromatics can cause health issues in human being and hence, it is necessary to detect and degrade nitroaromatic compounds for the sake of human safety and security [1, 2]. The byproducts generated from explosives, herbicides, insecticides and leather industries are mainly nitroaromatic compounds and are discharged into the environment [3, 4]. The presence of nitro group in benzene ring has stronger electron withdrawing tendency which attracts the electron density towards itself and makes the molecule more stable. The stable nature of nitrobenzene and its derivatives makes them as the unavoidable pollutant when they enter the soil or water. The nitrobenzene reduction has gained much importance for the creation of safer environment [5]. However, nitrobenzene oxidation can produce picolinic acid as dead end product which is more toxic [6]. Considering the toxic products in the oxidation of nitrobenzene, reduction technologies have received greater attention than oxidation [7]. Based on the different principles and techniques, various methodologies have been adopted for the detection of nitroaromatic compounds [8]. Various analytical techniques, such as, spectrophotometry [9, 10], gas chromatography [11], capillary electrophoresis [12] and high performance liquid chromatography [13] has been carried out for the determination of nitroaromatics. Owing to their high sensitivity, selectivity, simplicity and low-cost instrumentation, electrochemical-techniques based sensors are found to be promising for the detection of nitroaromatics [14–16]. Another advantage of employing electrochemical technique is that the electrochemical reduction of nitrobenzene generates less toxic compounds, such as, aniline, phenylhydroxylamine, azoxybenzene, azobenzene and nitrosobenzene [17]. Metal nanoparticles, like, silver nanoparticles (AgNPs) [14, 18] and gold nanoparticles (AuNPs) [19], modified electrodes have been employed as electrochemical sensors for the detection of nitrobenzene

(NB) and nitrobenzene derivatives. Bimetal Au/Ag nanorods modified electrode also used for the electrocatalytic reduction of nitrobenzene [20].

Transition metal nanoparticles exhibit excellent catalytic and electrocatalytic activity than the corresponding bulk materials [21]. The size and shape of metal nanoparticles determine the exceptional physical, chemical characteristics and their applicability in catalysis and sensors. Among the various transition metals, silver has the advantages like, high electrical conductivity and low-cost than others [22–23]. Hence, silver nanoparticles are extremely beneficial in catalytic and electrocatalytic applications. However, the stability of nanoparticles is a big issue due to the unsuitable high surface energy of the particles, which results in agglomeration of smaller nanoparticles. Various support materials, such as, SiO_2 [24], graphene oxide [25], reduced graphene oxide [26], carbon nanotubes [27] and TiO_2 [28] are investigated. Graphite like carbon nitride (g-C_3N_4), a medium bandgap semiconductor nanomaterial, draws wide consideration owing to its interesting nature. The low density, thermal constancy and medium bandgap of g-C_3N_4 make it as a potential candidate for light induced processes [29], hydrogen storage [30], lithium-ion battery [31], electrogenerated chemiluminescence [32] and fluorescent sensor [33]. But, the bulk g-C_3N_4 with poor water solubility and large size is not suitable for electrochemical sensing application. However, the large surface area (~ 300 m^2 g^{-1}) and good chemical stability of nanostructured g-C_3N_4 make it as a good support material and suitable candidate for electrochemical applications. AgNPs deposited g-C_3N_4 sheets were employed as electrocatalyst in the non-enzymatic detection of hydrogen peroxide and glucose [34] as well as in the reduction of oxygen [35].

In the present investigation, silver nanoparticles (AgNPs) decorated N-[3-(trimethoxysilyl)propyl]ethylenediamine (EDAS) modified graphitic carbon nitride nanocomposites (EDAS/(g-C_3N_4-Ag)$_{NC}$) are prepared through a simple reduction method. The electrochemical performances of the nanocomposites toward the electrocatalytic reduction of nitrobenzene and nitrobenzene derivatives have been investigated through cyclic voltammetry (CV) and square wave voltammetry (SWV) techniques.

2. Experimental Section

2.1. Chemicals

Urea, N-[3-(trimethoxysilyl)propyl]ethylenediamine (EDAS) and silver nitrate ($AgNO_3$) were obtained from Sigma-Aldrich, India. Sodium borohydride ($NaBH_4$), sodium dihydrogen phosphate, disodium hydrogen phosphate, nitrobenzene (NB), nitroaniline (NA), nitrobenzoic acid (NBA), nitrophenol (NP) and nitrotoluene (NT) were purchased from Merck, India. The purities of chemicals were of analytical grades. All the glasswares were treated with Aqua regia (1:3 HNO_3/HCl (v/v)) before carrying out experiments.

2.2. Preparation of EDAS/(g-C_3N_4-Ag)$_{NC}$

The procedure adopted for the preparation of g-C_3N_4 nanosheets is provided in Supplementary Information [36]. EDAS/(g-C_3N_4-Ag)$_{NC}$ was prepared as follows: 25 µL of EDAS was mixed with 2 mL of g-C_3N_4 nanosheets and stirred for 1 h. Into this mixture, 20 µL of $AgNO_3$ (0.1 M) solution were poured to maintain 1 mM concentration of $AgNO_3$ and stirred for another one hour. 100 µL of freshly prepared 0.1 M $NaBH_4$ was then added drop-wise into the above mixture in order to reduce $AgNO_3$. When the Ag^+ is reduced to Ag^0, the color of the reaction mixture turned to brownish yellow and it was left overnight so as to uniformly deposit the AgNPs on g-C_3N_4 nanosheets. The aggregation of AgNPs on g-C_3N_4 is prevented through amine group stabilization by EDAS. The prepared nanocomposite was centrifuged and washed with double distilled water to remove the unreduced $AgNO_3$ and $NaBH_4$. Finally, the product was redispersed in 2 mL of distilled water. Other two composites with $AgNO_3$ concentration of 2 mM and 3 mM were prepared by adding 40 and 60 µL of 0.1 M $AgNO_3$ solutions, keeping all other procedure same, for getting EDAS/(g-C_3N_4-Ag)$_{NC}$ with various amounts of AgNPs. Pictorial description of the nanocomposite preparation is shown in Scheme 1.

2.3. Characterization techniques

Diffuse reflectance spectra of the films were carried out using a Shimadzu UV-2550 (Shimadzu, Japan) UV-vis spectrophotometer fitted with ISR-2200 DRS accessory. The colloidal samples were coated on glass plate, dried completely and used for diffused reflectance studies. The scanning electron microscopy (SEM) and energy dispersive X-ray (EDX) analyses were performed by employing a FEI-QUANTA 250 high resolution scanning electron microscope. The high resolution transmission electron microscopic (HRTEM) images were recorded in a JEOL 3010 (Jeol, Japan) high resolution transmission electron microscope at an accelerating voltage of 200 kV. The specimen to be analyzed was dispersed in a solvent and coated onto carbon coated copper grid and dried in vacuum condition. The IR spectra analysis was carried using Shimadzu IRTRACER-100 (Shimadzu, Japan) FT-IR spectrophotometer. Cyclic voltammetry (CV) and square wave voltammetry (SWV) experiments were conducted in a single compartment three electrode cell using a electrochemical workstation (CH Instruments, USA, Model 680) at 25°C, by employing modified glassy carbon electrode (GCE) (CH instruments) as working electrode (area 0.07 cm^2), Ag/AgCl electrode as reference electrode and Pt wire as counter electrode.

2.4. Preparation of modified electrode and electrochemical studies

The electrochemical detection of nitrobenzene derivatives were conducted in a three electrode cell system containing phosphate buffer (pH 7.4) as a supporting electrolyte in nitrogen environment. 5 µL of EDAS/(g-C_3N_4-Ag)$_{NC}$ was coated on a polished and pre-cleaned glassy carbon (GC) electrode (disc shaped, 3 mm dia, area 0.07 cm^2). The modified electrode was dried for an hour at room temperature (~ 32°C) and utilized as a working electrode. Thin films on GC electrode were prepared using 2, 4, 5, 6 and 7 µL of EDAS/(g-C_3N_4-Ag)$_{NC}$ sol for optimization. As the electrode prepared using 5 µL exhibited

continuous stable film (< 5 µL gave discontinuous films; 7 µL showed aggregation) and maximum cyclic voltammetric current response, it was chosen for further studies. Platinum (Pt) wire and Ag/AgCl electrode were chosen as counter and reference electrodes, respectively. The square wave voltammograms were recorded (using CH Instruments, Model 680) by applying a step potential of 4 mV, amplitude of 25 mV and a frequency of 15 Hz. Experiments were done in triplicates and the average values are reported.

3. Results And Discussion

3.1. Characterization of EDAS/(g-C_3N_4-Ag)$_{NC}$

The formation of EDAS/(g-C_3N_4-Ag)$_{NC}$ was initially verified through UV-visible diffused reflectance spectra. The spectra of g-C_3N_4 nanosheets and (EDAS/g-C_3N_4-Ag)$_{NC}$ are depicted in Fig. 1. The presence of g-C_3N_4 nanosheets in the nanocomposite is confirmed from the typical UV-vis absorption edge near 430 nm. A new band appeared around 450 nm along with the typical absorption of g-C_3N_4 in EDAS/(g-C_3N_4-Ag)$_{NC}$ samples confirmed the formation of AgNPs on g-C_3N_4 nanosheets. The new band is attributed to the surface plasmon resonance (SPR) absorption characteristic of AgNPs.

Figure 2 shows the FT-IR spectra of g-C_3N_4 nanosheets and EDAS/(g-C_3N_4-Ag(2 mM))$_{NC}$ in the wave number range of 500–4000 cm^{-1}. The peak obtained in the range of 1240–1643 cm^{-1} is attributed to the characteristic stretching modes of C–N heterocycles. The broad absorption peaks appeared in the range of 3040 and 3300 cm^{-1} are ascribed to the N–H vibration and H_2O adsorption, respectively [37, 38]. The FT-IR data inferred that the attachment of Ag nanoparticles does not affect the structural features of the g-C_3N_4 nanosheets.

Figure 3 shows TEM images of the prepared EDAS/(g-C_3N_4-Ag(2 mM))$_{NC}$. The sheet-like structure of g-C_3N_4 suggests the presence of exfoliated g-C_3N_4 (Fig. 3 (A)). A large number of spherical AgNPs with size range of 10–15 nm are found on the g-C_3N_4 nanosheets surface, which confirmed the formation of AgNPs-loaded g-C_3N_4 nanosheets (Fig. 3(B)). The lattice fringes with interplanar distance of 0.235 nm assigned to Ag(111) facet was found on the AgNPs. The elemental characterization of EDAS/(g-C_3N_4-Ag(2 mM))$_{NC}$ was performed through EDX analysis (Fig. S1). The spectrum confirmed the presence of the elements C, N, O, Si and Ag by showing their X-ray lines. The elemental mapping of EDAS/(g-C_3N_4-Ag(2 mM))$_{NC}$ showed the uniform distribution of AgNPs in the nanocomposite and confirmed the formation of g-C_3N_4-Ag nanocomposite in EDAS sol-gel network (Fig. S1). Cyclic voltammogram of EDAS/(g-C_3N_4-Ag)$_{NC}$ modified electrode (Fig. S2) shows an anodic peak representing Ag oxidation at 0.23 V, which affirm the Ag presence in the composite material [39].

3.2. Electrocatalytic reduction of nitrobenzene (NB)

The electrocatalytic reduction of NB at the EDAS/(g-C_3N_4-Ag(2 mM))$_{NC}$ modified electrode (thin films over flat bottom of 3 mm dia GC electrode) was investigated through cyclic voltammetry. The cyclic voltammograms (CVs) recorded for 500 μM of NB at bare GC, GC/(EDAS/g-C_3N_4) and GC/EDAS/(g-C_3N_4-Ag(2 mM))$_{NC}$ modified electrodes at a scan rate of 50 mV s^{-1} are shown in Fig. 4. In the reductive scan with the GC/EDAS/(g-C_3N_4-Ag(2 mM))$_{NC}$ modified electrode, the reduction peak for nitrobenzene was observed at −0.68V, whereas, the corresponding oxidation peak was observed at 0.6 V. The reduction peak of NB in the bare GC and GC/(EDAS/g-C_3N_4) were observed at −0.78 V and −0.74 V, respectively. The reduction peak current of nitrobenzene for GC/EDAS/(g-C_3N_4-Ag(2 mM))$_{NC}$, GC/(EDAS/g-C_3N_4) and bare GC were found to be 22.22 μA, 7.2 μA and 8 μA, respectively. The above results imply that the GC/EDAS/(g-C_3N_4-Ag(2 mM))$_{NC}$ possesses enhanced electrocatalytic activity towards reduction of nitrobenzene.

Figure 5 depicts the CVs of GC/EDAS/(g-C_3N_4-Ag(1 mM))$_{NC}$, GC/EDAS/(g-C_3N_4-Ag(2 mM))$_{NC}$ and GC/EDAS/(g-C_3N_4-Ag(3 mM))$_{NC}$ modified electrodes in the presence of 0 μM to 600 μM nitrobenzene. Upon increasing the concentration of nitrobenzene, linear increase in the cathodic peak current is observed. For comparing the electrocatalytic reduction of nitrobenzene in different electrodes, the plots of cathodic peak current (I_{pc}) vs concentration of nitrobenzene obtained for various electrodes are shown in Fig. 5(d). It can be clearly visible that, the GC/EDAS/(g-C_3N_4-Ag(2 mM))$_{NC}$ modified electrode showed improved electrocatalytic activity than those of GC/EDAS/(g-C_3N_4-Ag(1 mM))$_{NC}$ and GC/EDAS/(g-C_3N_4-Ag(3 mM))$_{NC}$. Since the GC/EDAS/(g-C_3N_4-Ag(2 mM))$_{NC}$ modified electrode exhibited better activity, it was used for further electrochemical experiments.

Fig. S3 demonstrates the effect of pH on the electro-reduction of 0.5 mM nitrobenzene at GC/EDAS/(g-C_3N_4-Ag(2 mM))$_{NC}$ modified electrode. The peak potential for nitrobenzene reduction is shifted towards negative potentials on increasing the pH of the solution. It is evident that the negative shift of peak potential advocates the electron transfer and proton transfer occurs simultaneously. An increasing trend is observed in the cathodic peak current upto to pH 7.4 and tend to drop beyond that pH (pH>7.4). As the maximum peak current was attained at pH 7.4, it was fixed for sensor applications.The variation of scan rate on the electrocatalytic reduction of 0.5 mM nitrobenzene at GC/EDAS/(g-C_3N_4-Ag(2 mM))$_{NC}$electrode is displayed in Fig. S4.While increasing the scan rate from 10 to 300 mV s^{-1}, well-defined cathodic peak appears at −0.64 V. The value of current increased with increasing scan rate. Due to the irreversible nature of nitrobenzene reduction, the cathodic peak shifts toward more negative potential with increasing scan rate. A linear plot is obtained between the peak current and square root of the scan rate, which is depicted in Fig. S4 and it suggests that the reduction of nitrobenzene was a diffusion controlled process.

The mechanism of electroreduction of nitrobenzene may be understood from the scrutiny of CV recorded for the reduction of NB (500 μM) on the GC/EDAS/(g-C_3N_4-Ag(2 mM))$_{NC}$ modified electrode shown in Fig. S5. The peak obtained at −0.65 V is corresponding to the reduction of $-NO_2$ group to −NHOH group and an anodic peak at + 0.05 V is due to the oxidation of −NHOH to −NO group. A new peak observed at −

0.11 V in the second cycle may be ascribed to the reduction of –NO to –NHOH (Fig. 6) [17, 40]. The electrocatalytic activity of GC/EDAS/(g-C_3N_4-Ag(2 mM))$_{NC}$ was also evaluated in the presence of nitrobenzene derivatives. The well resolved peaks and very good electrochemical responses observed for the electroreduction of nitrobenzene derivatives at the modified electrode indicated that this modified electrode is capable of sensing nitrobenzene derivatives by its electroreducing property. The present GC/EDAS/(g-C_3N_4-Ag(2 mM))$_{NC}$ showed peak potential of −0.8 V, −0.67 V, 0.78 V and −0.7 V for the reduction of nitroaniline, nitrobenzoic acid, nitrophenol and nitrotoluene, respectively (Fig. S6). Upon increasing the concentration of analytes, linear increase in peak current is observed, revealing good sensing response of the GC/EDAS/(g-C_3N_4-Ag)$_{NC}$ electrode.

3.3. SWVs of NB on GC/EDAS/(g-C_3N_4-Ag (2 mM))$_{NC}$

The sensing ability of the GC/EDAS/(g-C_3N_4-Ag(2 mM))$_{NC}$ modified electrode (thin films over flat bottom of 3 mm dia GC electrode) towards the detection of nitrobenzene and its derivatives was investigated by SWV. The square wave voltammograms (SWVs) were recorded by applying a step potential of 4 mV, amplitude of 25 mV and a frequency of 15 Hz. The SWV curve obtained for each addition of 5 µM nitrobenzene at the GC/EDAS/(g-C_3N_4-Ag(2 mM))$_{NC}$ modified electrode is shown in Fig. 7(A). The cathodic peak for NB reduction appears at −0.58V. While increasing the concentration of nitrobenzene, linear increase in the current is observed. The modified electrode also exhibits better responses for the addition of 2 µM nitrobenzene which is shown in Fig. 7(B).

The SWV signals obtained for the determination of nitrobenzoic acid (NBA), nitroaniline (NA), nitrophenol (NP) and nitrotoluene (NT), employing the GC/EDAS/(g-C_3N_4-Ag (2 mM))$_{NC}$ modified electrode, at each increase of 5 µM nitrobenzene derivatives are shown in Fig. 8. The modified electrode performed well with moderate concentrations of NBA, NA, NP and NT (Fig. 8). Due to the adsorption of redox analytes at higher concentration of analytes, a split in square wave voltammograms is observed [41, 42].

Table 1 summarizes the results obtained with various electroanalytical techniques and different metal nanocomposite electrodes including EDAS/(g-C_3N_4-Ag)$_{NC}$ modified electrode for the determination of NB and its derivatives [8, 24, 43–53]. The abbreviations of the modified electrodes in the table are given as provided in the appropriate references. The prepared EDAS/(g-C_3N_4-Ag)$_{NC}$ showed relatively low LOD and wide sensing range, mainly owing to the synergy of AgNPs and g-C_3N_4 nanosheets.

Table 1
Comparison of LOD for nitrobenzene at EDAS/$(g\text{-}C_3N_4\text{-}Ag)_{NC}$ with other reported modified electrodes.

Electrode material	Analyte	Analytical Technique	Detection limit	Ref
GC/EDAS-AgNPs	Nitrobenzene	Amperometry	2.5 nM	[8]
GC/TPDT-SiO_2/AgNPs	Nitrobenzene	SWV	0.5 μM	[24]
GC/GO	p-Nitrophenol	LSV	0.02 μM	[43]
GC/nano-gold	p-Nitrophenol Semi-derivative	Voltammetry	8 μM	[44]
CPE/CD-SBA	p-Nitrophenol	DPV	0.01 μM	[45]
GC/Pt-PdNPs/CNTs-rGO	Nitrobenzene	DPV	0.42 ppb	[46]
GC/Pt-PdNPs/CNTs-rGO	p-Nitroaniline	DPV	0.62 ppb	[46]
CPE/DTD/AgNPs	p-Nitroaniline	DPV	0.23 μM	[47]
GC/OMCN-800	Nitrobenzene	DPV	0.18 μM	[48]
GC/po-MWCNTs	p-Nitrotoluene	SWASV	0.28 μM	[49]
GC/pn-MWCNTs	p-Nitrotoluene	SWASV	0.442 nM	[49]
GC/γ-Al_2O_3	Nitrobenzene	DPV	0.15 μM	[50]
GC/AuNPs	Nitrobenzene	DPV	0.016 μM	[51]
OMC/DDAB/GC	Nitrobenzene	LSV	10 μM	[52]
β-$CD_{1.2mg}$/GO/SPCE	Nitrobenzene	LSV	0.184 μM	[53]
GC/EDAS/$(g\text{-}C_3N_4\text{-}Ag)_{NC}$	Nitrobenzene	SWV	2 μM	Present work

4. Conclusions

The EDAS/$(g\text{-}C_3N_4\text{-}Ag)_{NC}$ with different silver concentrations were prepared using a simple reduction method. The UV-vis absorption edge at 430 nm together with a broad SPR peak at 450 nm confirm that the AgNPs are attached to the g-C_3N_4 nanosheets surface. The characteristic stretching modes of C–N heterocycles observed in the FT-IR spectra affirmed the presence of g-C_3N_4 nanosheets in the composite. The presence of Ag in EDAS/$(g\text{-}C_3N_4\text{-}Ag)_{NC}$ was further confirmed by EDX analysis and cyclic voltammetry. TEM analysis established that the so-formed AgNPs on g-C_3N_4 nanosheets are in the size range of 10–15 nm. The prepared nanocomposite forms a stable thin film over GC electrode to give highly active modified electrode. The EDAS/$(g\text{-}C_3N_4\text{-}Ag)_{NC}$ with 2 mM silver concentration showed very

good electroactivity towards the reduction of NB and its derivatives, delivering lowest experimental detection limit of 2 μM for NB. Further improvement in the LOD for NB and its derivatives by incorporating bi-metal nanoparticles, like, Ag/Cu or Ag/Au into g-C_3N_4 shall be explored, as it has great potential in electrochemical sensing of trace nitrobenzene.

Declarations

Declaration of interests

The authors have no conflicts of interest to declare.

Acknowledgements

CP is a beneficiary of Junior/Senior Research Fellowship from University Grants Commission, India. The authors also thank R. Praveen for his timely help. M. Selvaraj is grateful to Deanship of Scientific Research, King Khalid University for funding through Large Research Group Project (No. R.G.P. 2/139/1442).

References

1. S. Hrapovic, E. Majid, Y. Liu, K. Male, J.H.T. Luong, Metallic nanoparticle – carbon nanotube composites for electrochemical determination of explosive nitroaromatic compounds. Anal. Chem. **78**, 5504–5512 (2006)
2. B.K. Ong, H.L. Poh, C.K. Chua, M. Pumera, Graphenes prepared by Hummers, Staudenmaier and Hofmann methods for analysis of TNT-based nitroaromatic explosives in seawater. Electroanal. **24**, 2085–2093 (2012)
3. D. Cropek, P.A. Kemme, O.V. Makarova, L.X. Chen, T. Rajh, Selective photocatalytic decomposition of nitrobenzene using surface modified TiO_2 nanoparticles. J. Phys. Chem. C **112**, 8311–8318 (2008)
4. A.M. O'Mahony, J. Wang, Nanomaterial-based electrochemical detection of explosives: a review of recent developments. Anal. Methods **5**, 4296–4309 (2013)
5. S. Singh, Sensors–An effective approach for the detection of explosives. J. Hazard. Mater. **144**, 15–28 (2007)
6. S.F. Nishino, J.C. Spain, Degradation of nitrobenzene by a Pseudomonas pseudoalcaligenes. Appl. Environ. Microbiol. **59**, 2520–2525 (1993)
7. E.K. Nefso, S.E. Burns, C.J. McGrath, Degradation kinetics of TNT in the presence of six mineral surfaces and ferrous iron. J. Hazard. Mater. **123**, 79–88 (2005)
8. G. Maduraiveeran, R. Ramaraj, Potential sensing platform of silver nanoparticles embedded in functionalized silicate shell for nitroaromatic compounds. Anal. Chem. **81**, 7552–7560 (2009)
9. A. Niazi, A. Yazdanipour, Spectrophotometric simultaneous determination of nitrophenol isomers by orthogonal signal correction and partial least squares. J. Hazard. Mater. **146**, 421–427 (2007)

10. W. Zhang, C.R. Wilson, N.D. Danielson, Indirect fluorescent determination of selected nitro-aromatic and pharmaceutical compounds via UV-photolysis of 2-phenylbenzimidazole-5-sulfonate. Talanta **74**, 1400–1407 (2008)
11. J.A. Padilla-Sanchez, P. Plaza-Bolanos, R.R. -Gonzalez, A.G. -Frenich, J.L.M. Vidal, Application of a quick, easy, cheap, effective, rugged and safe-based method for the simultaneous extraction of chlorophenols, alkylphenols, nitrophenols and cresols in agricultural soils, analyzed by using gas chromatography–triple quadrupole-mass spectrometry/mass spectrometry. J. Chromatogr. A **1217**, 5724–5731 (2010)
12. X. Guo, Z. Wang, S. Zhou, The separation and determination of nitrophenol isomers by high-performance capillary zone electrophoresis. Talanta **64**, 135–139 (2004)
13. D. Hofmann, F. Hartmann, H. Herrmann, Analysis of nitrophenols in cloud water with a miniaturized light-phase rotary perforator and HPLC-MS. Anal. Bioanal. Chem. **391**, 161–169 (2008)
14. G. Kortum, *Treatise on Electrochemistry* (Elsevier Pub. Co., Amsterdam, 1965), p. 497
15. H.X. Zhang, A.M. Cao, J.S. Hu, L.J. Wan, S.T. Lee, Electrochemical sensor for detecting ultratrace nitroaromatic compounds using mesoporous SiO_2-modified electrode. Anal. Chem. **78**, 1967–1971 (2006)
16. J.C. Chen, J.L. Shih, C.H. Liu, M.Y. Kuo, J.M. Zen, Disposable electrochemical sensor for determination of nitroaromatic compounds by a single-run approach. Anal. Chem. **78**, 3752–3757 (2006)
17. Y.P. Li, H.B. Cao, C.M. Liu, Y. Zhang, Electrochemical reduction of nitrobenzene at carbon nanotube electrode. J. Hazard. Mater. **148**, 158–163 (2007)
18. S. Manivannan, R. Ramaraj, Silver nanoparticles embedded in cyclodextrin–silicate composite and their applications in Hg(II) ion and nitrobenzene sensing. Analyst **138**, 1733–1739 (2013)
19. S. Manivannan, R. Ramaraj, Synthesis of cyclodextrin-silicate sol–gel composite embedded gold nanoparticles and its electrocatalytic application. Chem. Eng. J. **210**, 195–202 (2012)
20. S. Jayabal, R. Ramaraj, Bimetallic Au/Ag nanorods embedded in functionalized silicate sol–gel matrix as an efficient catalyst for nitrobenzene reduction. Appl. Catal. A **470**, 369–375 (2014)
21. A.P. Alivisatos, Semiconductor clusters, nanocrystals, and quantum dots. Science **271**, 933–937 (1996)
22. F. Bidault, A. Kucernak, A novel cathode for alkaline fuel cells based on a porous silver membrane. J. Power Sources **195**, 2549–2556 (2010)
23. C.M. Welch, C.E. Banks, A.O. Simm, R.G. Compton, Silver nanoparticle assemblies supported on glassy-carbon electrodes for the electro-analytical detection of hydrogen peroxide. Anal. Bioanal. Chem. **382**, 12–21 (2005)
24. P. Rameshkumar, R. Ramaraj, Electroanalysis of nitrobenzene derivatives and nitrite ions using silver nanoparticles deposited silica spheres modified electrode. J. Electroanal. Chem. **731**, 72–77 (2014)

25. J. Zhu, P. Xiao, H. Li, S.A.C. Carabineiro, Graphitic carbon nitride: synthesis, properties, and applications in catalysis. ACS Appl. Mater. Interfaces **6**, 16449–16465 (2014)
26. S. Rana, G.B.B. Varadwaj, S.B. Jonnalagadda, Ni nanoparticle supported reduced graphene oxide as a highly active and durable heterogeneous material for coupling reactions. Nanoscale Advances **1**, 1527–1530 (2019)
27. W. Zhang, P. Sherrell, A.I. Minett, J.M. Razal, J. Chen, Carbon nanotube architectures as catalyst supports for proton exchange membrane fuel cells. Ener. Environ. Sci. **3**, 1286–1293 (2010)
28. T. Froschl, U. Hormann, P. Kubiak, G. Kucerova, M. Pfanzelt, C.K. Weiss, R.J. Behm, N. Husing, U. Kaiser, K. Landfester, M.W. -Mehrens, High surface area crystalline titanium dioxide: potential and limits in electrochemical energy storage and catalysis. Chem. Soc. Rev. **41**, 5313–5360 (2012)
29. G. Dong, Y. Zhang, Q. Pan, J. Qiu, A fantastic graphitic carbon nitride (g-C_3N_4) material: electronic structure, photocatalytic and photoelectronic properties. J. Photochem. Photobiol. C: Photochem. Rev. **20**, 33–50 (2014)
30. A.A.S. Nair, R. Sundara, N. Anitha, Hydrogen storage performance of palladium nanoparticles decorated graphitic carbon nitride. Int. J. Hydrogen Energy **40**, 3259–3267 (2015)
31. J. Chen, Z. Mao, L. Zhang, D. Wang, R. Xu, L. Bie, B.D. Fahlman, Nitrogen-deficient graphitic carbon nitride with enhanced performance for lithium ion battery anodes. ACS Nano **11**, 12650–12657 (2017)
32. C. Cheng, Y. Huang, X. Tian, B. Zheng, Y. Li, H. Yuan, D. Xiao, S. Xie, M.M.F. Choi, Electrogenerated chemiluminescence behavior of graphite-like carbon nitride and its application in selective sensing. Cu^{2+}. Anal. Chem. **84**, 4754–4759 (2012)
33. C. Yang, X. Wang, H. Liu, S. Ge, J. Yu, M. Yan, On–off–on fluorescence sensing of glutathione in food samples based on a graphitic carbon nitride (g-C_3N_4)–Cu^{2+} strategy. New J. Chem. **41**, 3374–3379 (2017)
34. M.K. Kundu, M. Sadhukhan, S. Barman, Ordered assemblies of silver nanoparticles on carbon nitride sheets and their application in the non-enzymatic sensing of hydrogen peroxide and glucose. J. Mater. Chem. B **3**, 1289–1300 (2015)
35. L. Xu, H. Li, J. Xia, L. Wang, H. Xu, H. Ji, H. Li, K. Sun, Graphitic carbon nitride nanosheet supported high loading silver nanoparticle catalysts for the oxygen reduction reaction. Mater. Lett. **128**, 349–353 (2014)
36. L. Chen, X. Zeng, P. Si, Y. Chen, Y. Chi, D.-H. Kim, G. Chen, Gold nanoparticle-graphite-like C_3N_4 nanosheet nanohybrids used for electrochemiluminescent immunosensor. Anal. Chem. **86**, 4188–4195 (2014)
37. C.-Z. Li, Z.-B. Wang, X.-L. Sui, L.-M. Zhang, D.-M. Gu, Ultrathin graphitic carbon nitride nanosheets and graphene composite material as high-performance PtRu catalyst support for methanol electro-oxidation. Carbon **93**, 105–115 (2015)

38. Y. Zhang, M. Yan, S. Ge, C. Ma, J. Yu, X. Song, An enhanced photoelectrochemical platform: graphite-like carbon nitride nanosheet-functionalized ZnO nanotubes. J. Mater. Chem. B **4**, 4980–4987 (2016)
39. S. Manivannan, R. Ramaraj, Core-shell Au/Ag nanoparticles embedded in silicate sol-gel network for sensor application towards hydrogen peroxide. J. Chem. Sci. **121**, 735–743 (2009)
40. H.-X. Zhang, A.-M. Cao, J.-S. Hu, L.-J. Wan, S.-T. Lee, Electrochemical sensor for detecting ultratrace nitroaromatic compounds using mesoporous SiO_2-modified electrode. Anal. Chem. **78**, 1967–1971 (2006)
41. J.H. Reeves, S. Song, E.F. Bowden, Application of square wave voltammetry to strongly adsorbed quasireversible redox molecules. Anal. Chem. **65**, 683–688 (1993)
42. J.L. Lyon, K.J. Stevenson, Picomolar peroxide detection using a chemically activated redox mediator and square wave voltammetry. Anal. Chem. **78**, 8518–8525 (2006)
43. J. Li, D. Kuang, Y. Feng, F. Zhang, Z. Xu, M. Liu, A graphene oxide-based electrochemical sensor for sensitive determination of 4-nitrophenol. J. Hazard. Mater. **201–202**, 250–259 (2012)
44. L. Chu, L. Han, X. Zhang, Electrochemical simultaneous determination of nitrophenol isomers at nano-gold modified glassy carbon electrode. J. Appl. Electrochem. **41**, 687–694 (2011)
45. X. Xu, Z. Liu, X. Zhang, S. Duan, S. Xu, C. Zhou, β-Cyclodextrin functionalized mesoporous silica for electrochemical selective sensor: simultaneous determination of nitrophenol isomers. Electrochim. Acta **58**, 142–149 (2011)
46. C.X. Yuan, Y.R. Fan, T. Zhang, H.X. Guo, J.X. Zhang, Y.L. Wang, D.L. Shan, X.Q. Lu, A new electrochemical sensor of nitro aromatic compound based on three-dimensional porous Pt–Pd nanoparticles supported by graphene–multiwalled carbon nanotube composite. Biosens. Bioelectron. **58**, 85–91 (2014)
47. M.H.A. Zavar, S. Heydari, G.H. Rounaghi, H. Eshghi, H.A. Toupkanloo, Electrochemical behavior of para-nitroaniline at a new synthetic crown ether-silver nanoparticle modified carbon paste electrode. Anal. Methods **4**, 953–958 (2012)
48. Y. Zhang, X. Bo, A. Nsabimana, C. Luhana, G. Wang, H. Wang, M. Li, L. Guo, Fabrication of 2D ordered mesoporous carbon nitride and its use as electrochemical sensing platform for H_2O_2, nitrobenzene, and NADH detection. Biosens. Bioelectron. **53**, 250–256 (2014)
49. R. Yang, Y. Wei, Y. Yu, C. Gao, L. Wang, J.H. Liu, X.J. Huang, Make it different: the plasma treated multi-walled carbon nanotubes improve electrochemical performances toward nitroaromatic compounds. Electrochim. Acta **76**, 354–362 (2012)
50. B. Thirumalraj, S. Palanisamy, S.-M. Chen, K. Thangavelu, P. Periakaruppan, X.-H. Liu, A simple electrochemical platform for detection of nitrobenzene in water samples using an alumina polished glassy carbon electrode. J. Colloid Interface Sci. **475**, 154–160 (2016)
51. R. Emmanuel, C. Karuppiah, S.-M. Chen, S. Palanisamy, S. Padmavathy, P. Prakash, Green synthesis of gold nanoparticles for trace level detection of a hazardous pollutant (nitrobenzene) causing Methemoglobinaemia. J. Hazard. Mater. **279**, 117–124 (2014)

52. B. Qi, F. Lin, J. Bai, L. Liu, L. Guo, An ordered mesoporous carbon/didodecyldimethylammonium bromide composite and its application in the electro-catalytic reduction of nitrobenzene. Mater. Lett. **62**, 3670–3672 (2008)
53. M. Velmurugan, N. Karikalan, S.-M. Chen, Z.-C. Dai, Studies on the influence of β-cyclodextrin on graphene oxide and its synergistic activity to the electrochemical detection of nitrobenzene. J. Colloid Interface Sci. **490**, 365–371 (2017)

Figures

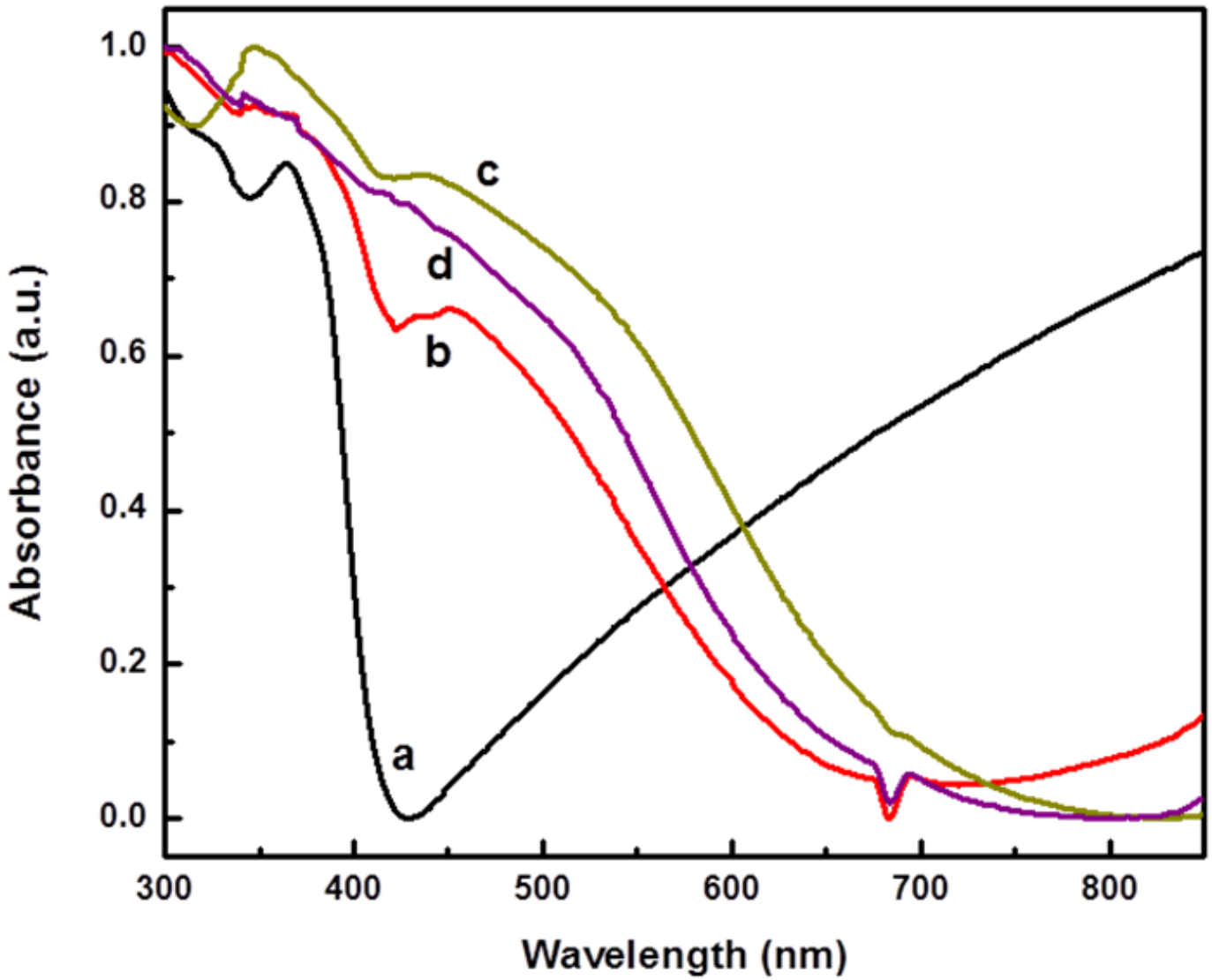

Figure 1

Diffuse reflectance spectra of (a) g-C3N4 nanosheets, (b) EDAS/(g-C3N4-Ag(1 mM))NC, (c) EDAS/(g-C3N4-Ag(2 mM))NC and (d) EDAS/(g-C3N4-Ag(3 mM))NC.

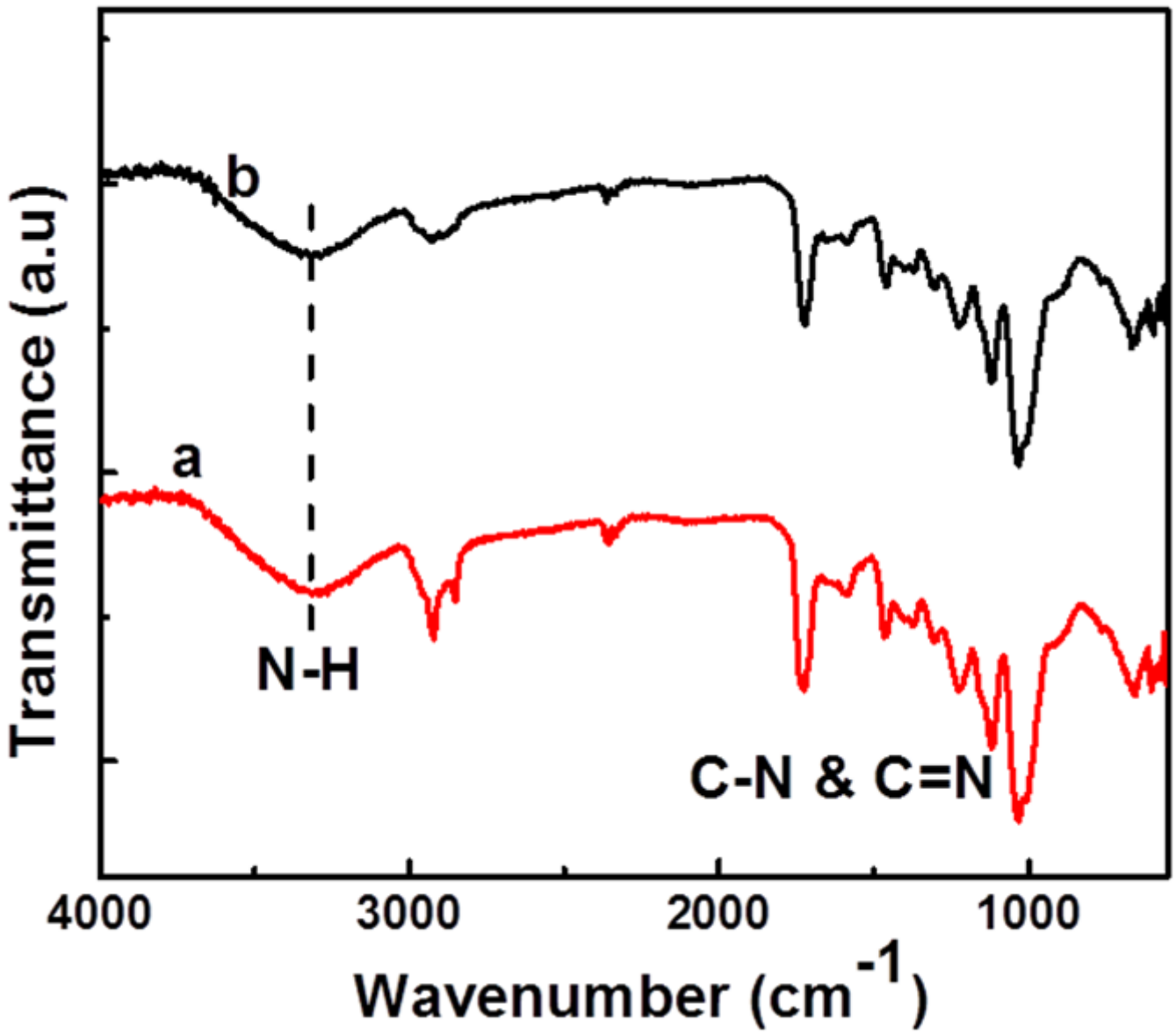

Figure 2

FT-IR spectra of (a) g-C3N4 nanosheets and (b) EDAS/(g-C3N4-Ag(2 mM))NC.

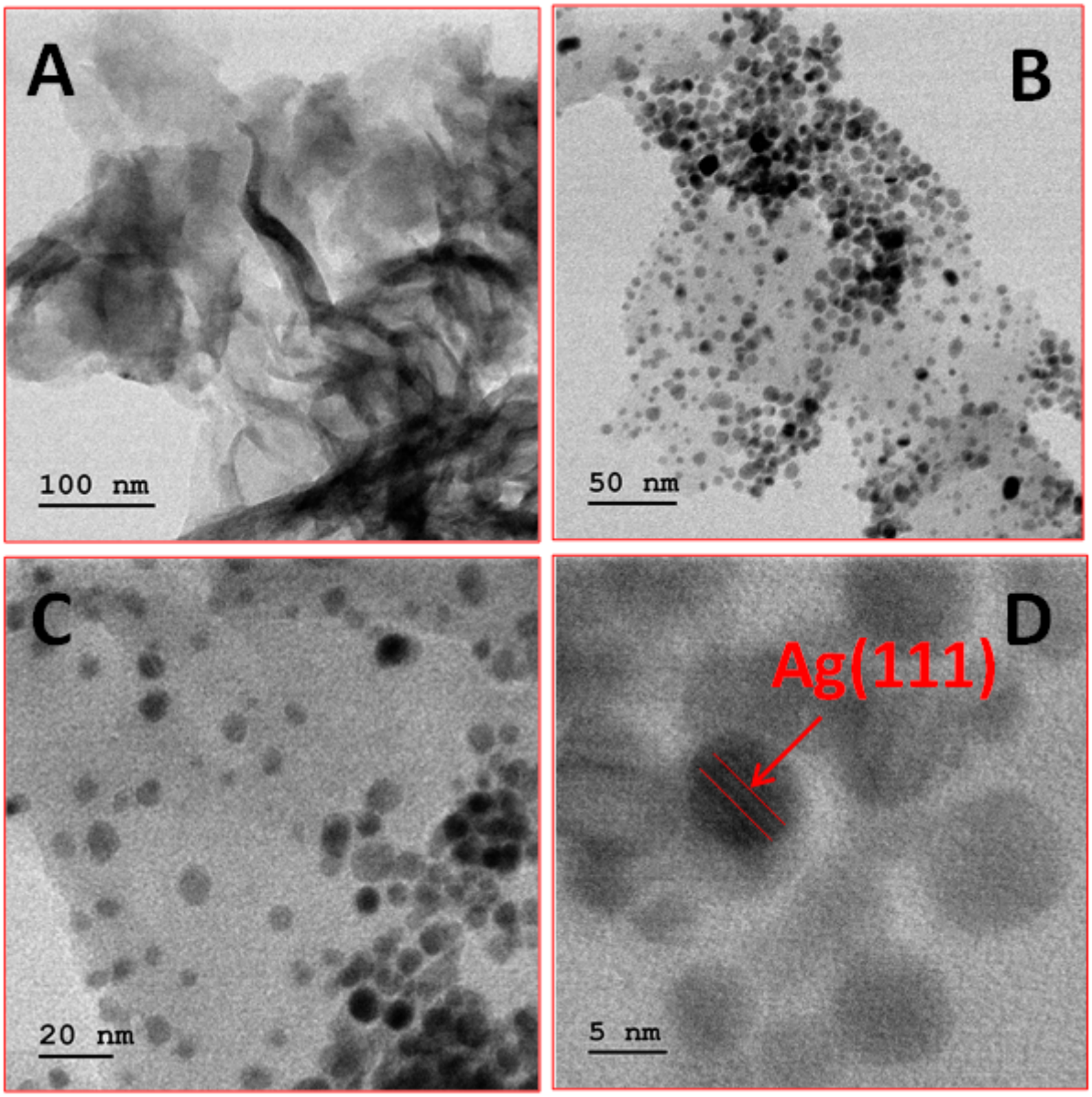

Figure 3

HRTEM images of (A) g-C3N4 and (B-D) EDAS/(g-C3N4-Ag(2 mM))NC.

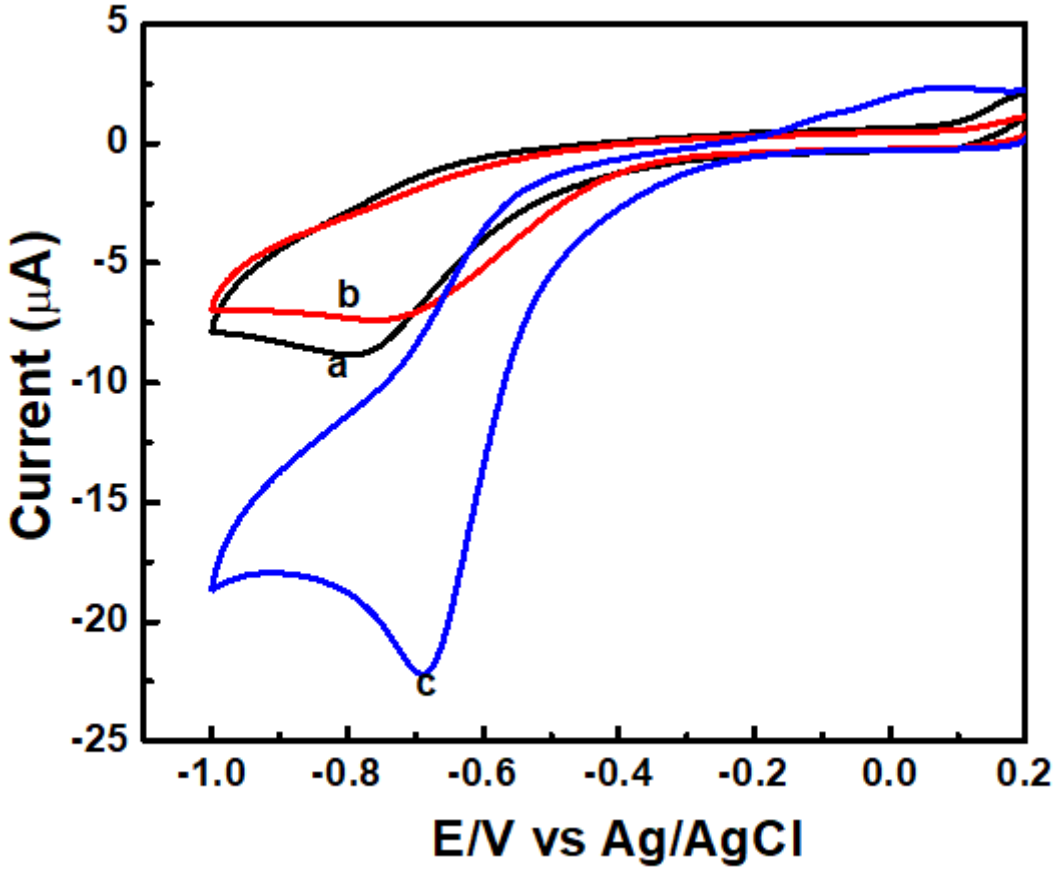

Figure 4

Cyclic voltammograms recorded for (a) bare GC, (b) GC/(EDAS/C3N4) and (c) GC/EDAS/(g-C3N4-Ag(2 mM))NC in the presence of 0.5 mM NB in 0.1 M PBS (pH 7.4) at a scan rate of 50 mV s−1.

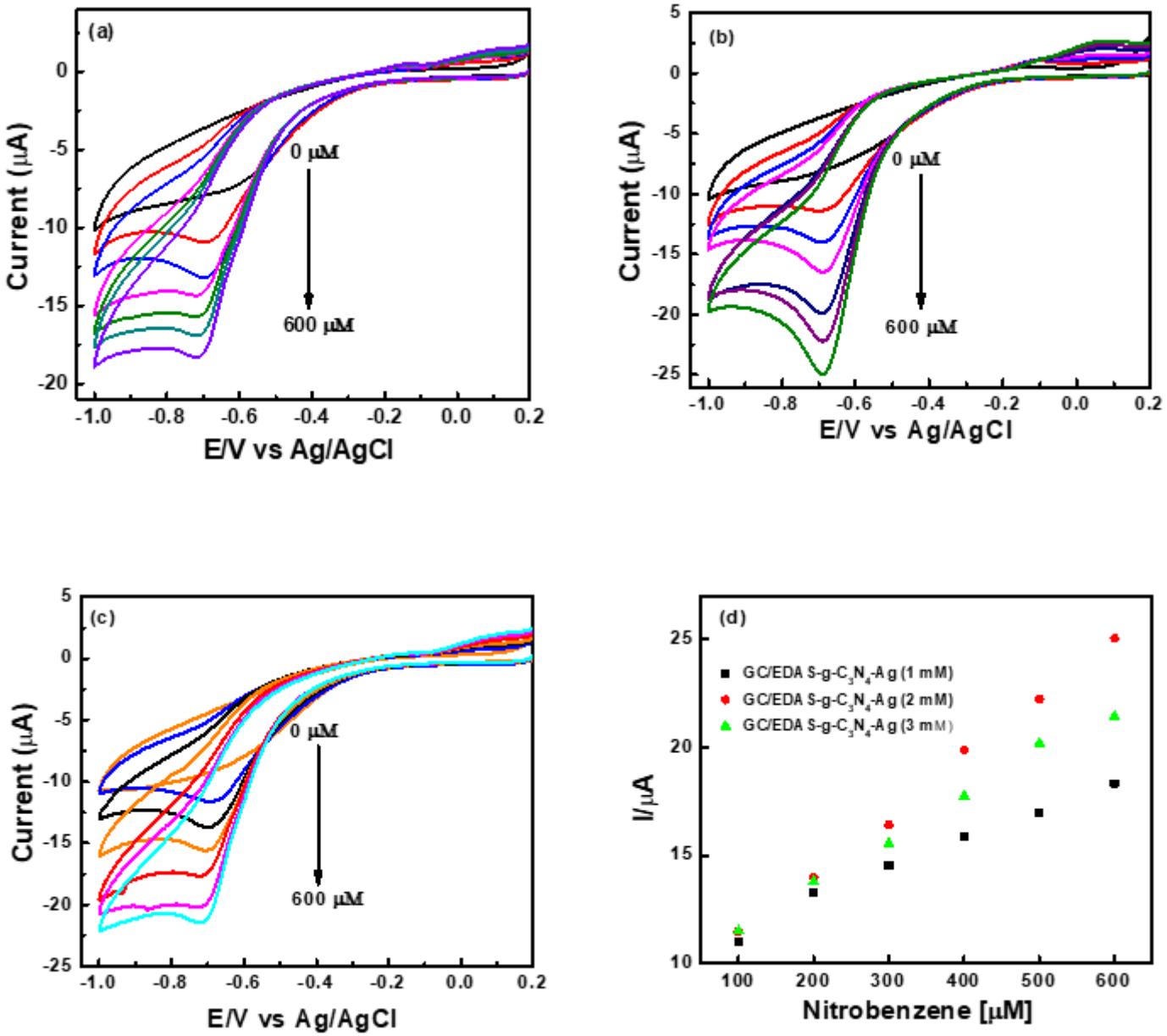

Figure 5

Cyclic voltammograms of (a) GC/EDAS/(g-C3N4-Ag(1 mM))NC (b) GC/EDAS/(g-C3N4-Ag(2 mM))NC and (c) GC/EDAS/(g-C3N4-Ag(3 mM))NC modified electrodes in 0.1 M PBS with various concentrations of NB (0 μM to 600 μM), and (d) corresponding calibration curves.

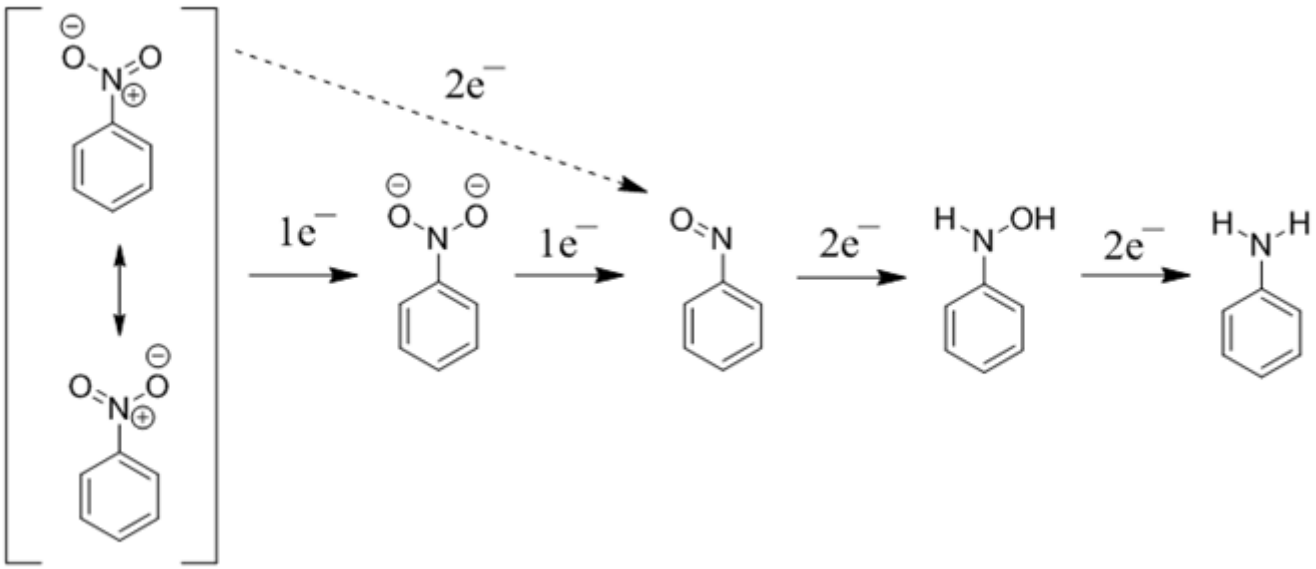

Figure 6

Mechanism for the reduction of nitro groups in nitroaromatic compounds [39].

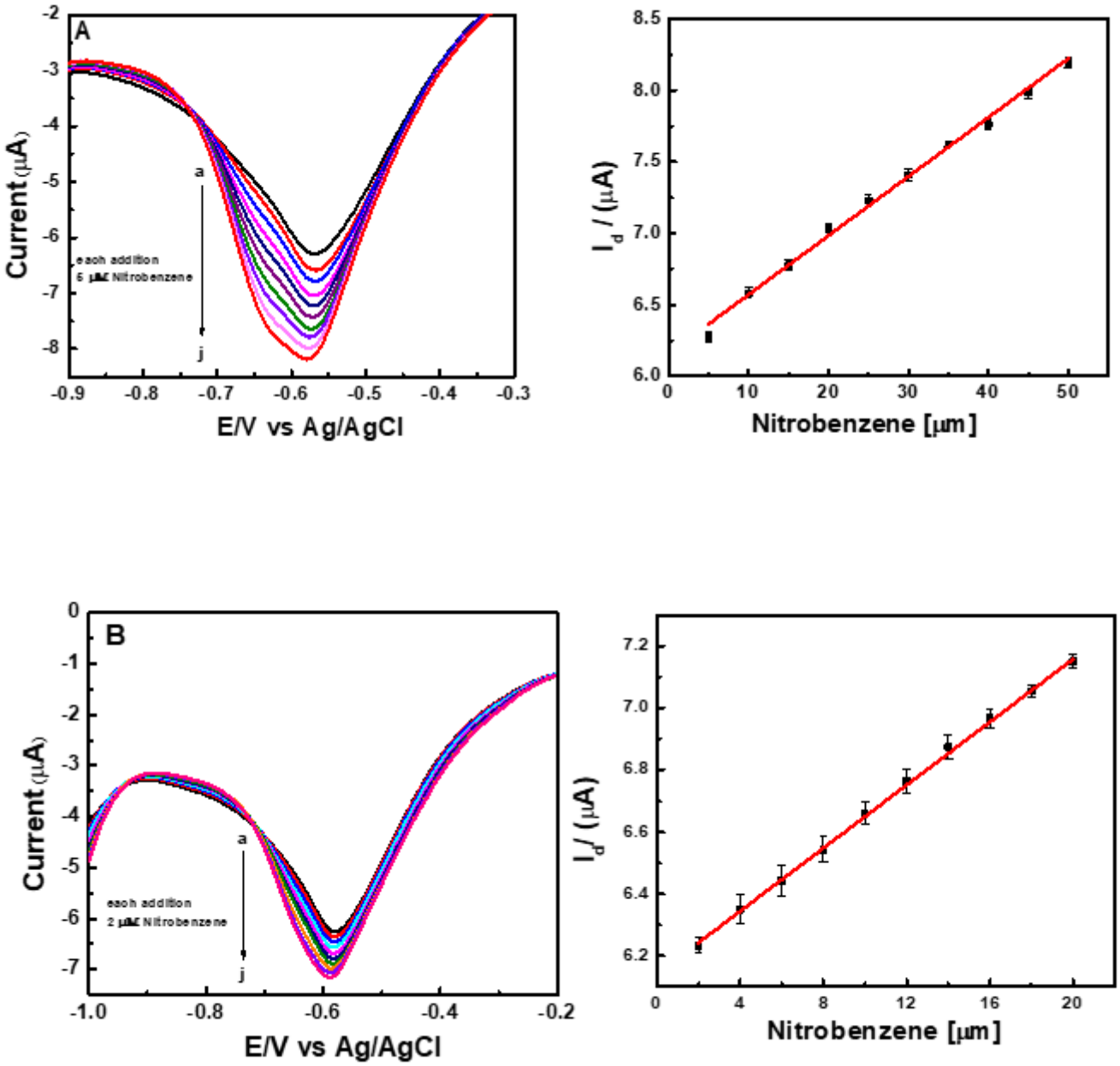

Figure 7

SWVs obtained for each increase of (A) 5 μM nitrobenzene (a = 5 to j = 50 μM) and (B) 2 μM nitrobenzene (a = 2 to j = 20 μM) at GC/EDAS/(g-C3N4-Ag(2 mM))NC electrode in 0.1 M PBS (pH 7.4), and their corresponding calibration plots (n = 3).

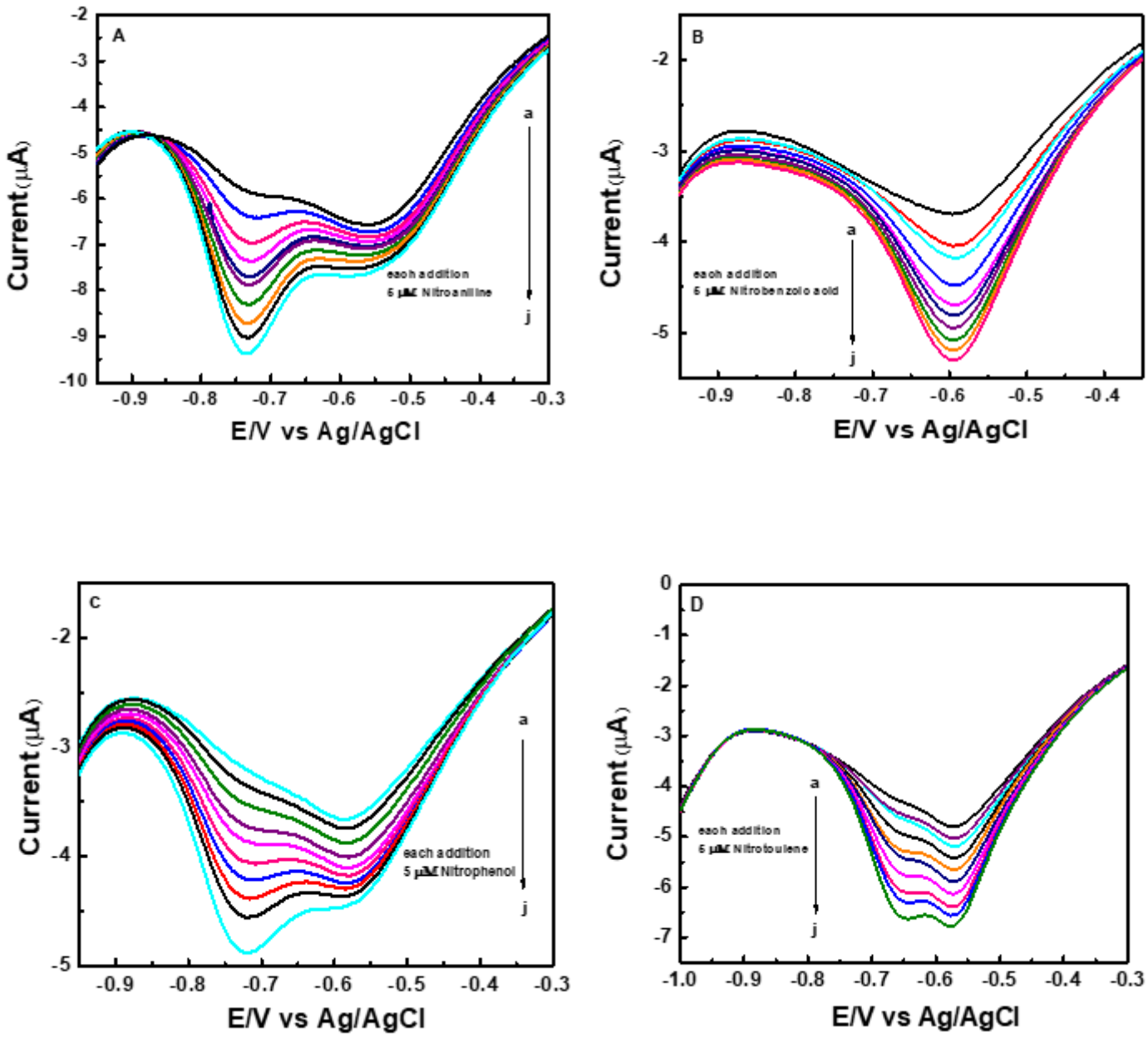

Figure 8

SWVs obtained at GC/EDAS/(g-C3N4-Ag(2 mM))NC electrode for each increase of 5 μM of (A) p-nitroaniline, (B) p-nitrobenzoic acid, (C) p-nitrophenol and (D) p-nitrotoluene, in 0.1 M PBS (pH 7.4); (a = 5 to j = 50 μM)

Supplementary Files

This is a list of supplementary files associated with this preprint. Click to download.

- schema1.png
- MSSupplementary.doc